3rd Specialty Conference on Material Engineering & Applied Mechanics
3e Conférence spécialisée sur le génie des matériaux et mécanique appliquée

Montréal, Québec
May 29 to June 1, 2013 / *29 mai au 1 juin 2013*

Experimental Testing of Conventional HSS Slotted Tube-to-Gusset Plate Connections Loaded Under Static and Dynamic Strain Rates

Rolando Moreau[1], Colin Rogers[1], Robert Tremblay[2]

[1]Department of Civil Engineering & Applied Mechanics, McGill University, Canada
[2]Department of Civil, Geological & Mining Engineering, Ècole Polytechnique, Canada

Abstract : Steel concentrically braced frames (CBFs) are popular seismic-force-resisting systems for low- to medium-rise buildings in Canada. Hollow structural section (HSS) members are commonly used for the lateral braces of these CBFs. HSS braces are often connected to the bracing-bent frames by using a slotted tube-to-gusset plate or knife-plate connection. This connection creates the potential under seismic loading for fracture of the tube through the net section, which can be further affected by shear lag. Shear lag factors calculated according to CSA S16 are quite penalizing, and can lead to expensive connection reinforcements when seismic capacity design methods must be applied. Furthermore, it is known that the yield stress of steel increases with strain rate; this places additional demand on the connection since it must be designed for the expected yield strength of the brace under seismic loading. However, strain-rate effects are typically ignored in design. This paper describes the testing of four HSS brace connections for HSS 152x152x9.5 and HSS 203x203x13.0 members under monotonic tensile loading. For each tube size, one brace was tested under a static rate, while the other brace was tested using a strain rate consistent with that which would occur during a design level earthquake. This paper reports on the applicability of existing design shear lag factors for square HSS sections, as well as the effect of strain rate on HSS brace connection behaviour.

1 INTRODUCTION

Steel concentrically braced frames (CBFs) are popular seismic-force-resisting systems (SFRS) for low- to medium- rise buildings in Canada due to their inherent strength, stiffness and economy. Hollow structural sections (HSS) or tubular members commonly form the bracing members for these CBFs. Slotted tube-to-gusset plate or knife-plate connections (Figure 1a) are often used to connect the HSS brace to a beam-to-column connection in a bracing bent. This connection detail is favoured by fabricators and designers due to its ease in design, fabrication and erection.

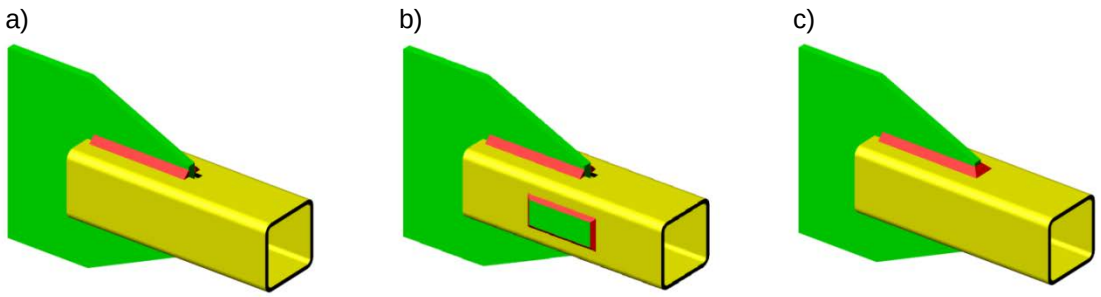

Figure 1: a) Conventional slotted tube-to-gusset plate connection, b) Connection reinforced with plate, c) Wrapped-around welds

However, this connection possesses two major weaknesses: net-section fracture and shear lag. The slot in the tube creates a reduced cross-sectional area, whereby a brittle tensile fracture can occur during an earthquake. This type of failure was observed during the 1995 Kobe earthquake (Tremblay et al. 1996) and during past experimental research programs (Yang and Mahin 2004, Fell and Kanvinde 2010).

In addition, shear lag diminishes a brace's net-section tension resistance; current shear lag design provisions are known to be conservative (Willibald et al. 2004). Subsequently, a designer has to often specify connection reinforcement when seismic capacity design methods are applied. Side reinforcement-plates (Figure 1b) can be welded to the brace, or wrapped-around welds (Figure 1c) can be specified to increase the area of the brace. However, side reinforcement-plates are expensive to fabricate, and wrapped-around welds are unreliable (AISC 2010a). For circular tubes, a special connection detail called the "Modified-Hidden-Gap (MHG)" (Martinez-Saucedo et al. 2008) may represent an economical and structurally attractive alternative to these connection reinforcements. A research program has been initiated to develop design and detailing rules for the MHG connection for square HSS bracing members. The first part of the program consists of examining existing design shear lag factors for square HSS members. Thus, this paper reports on the applicability of shear lag factors for square HSS members, as well as the influence of strain rate on brace connection behaviour.

2 LITERATURE REVIEW

2.1 Shear Lag

Shear lag is created as a result of using the slotted tube-to-gusset plate connection since the entire cross-sectional area of the HSS is not connected to the gusset plate. Shear lag results in an uneven strain distribution around the tube with the highest strains occurring where tube is welded directly onto the gusset plate. Net-section fracture often initiates at the beginning of the weld near the open slot and propagates circumferentially through the net area of the brace, A_n. Thus, the stress on the net area is non-uniform, and this is accounted for in CSA S16-09 Standard (CSA 2009a) by an effective net-area, A_{ne}. The shear lag factor, U, is defined as A_{ne}/A_n. Negligible shear lag is defined by a maximum U value of 1.0.

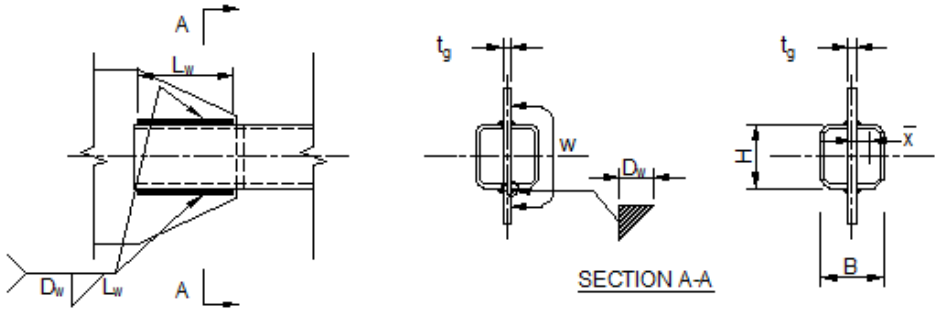

Figure 2: Definition of variables used to define shear lag

Table 1 summarizes the current design provisions used to account for shear lag in HSS members. CSA S16 defines shear lag in terms of L_w/w, where L_w is the weld length, and w is the circumferential distance between welds for one-half of the tube (Figure 2). On the other hand, AISC 360-10 (AISC 2010b) defines shear lag in terms of $\bar{x}/L_w$, where $\bar{x}$ represents the eccentricity for one-half of the tube with respect to the gusset plate center line (Figure 2). However, past experimental programs by Cheng and Kulak (2000) and Martinez-Saucedo (2007) have shown that the current shear lag factors found in the CSA S16 and AISC standards for circular HSS are overly conservative. Martinez-Saucedo (2007) has proposed an alternative shear lag equation for circular HSS sections (Table 1) which was based on experimental and numerical studies. According to this equation, U tends to 1.0 when L_w/w approaches 1.0.

Table 1: Comparison of Design Provisions used for Shear Lag

Specification	Shear-Lag Factors ($A_{ne} = UA_n$)	Range of Validity
CSA S16-09 Design of Steel Structures	$U = 1.0$, when $L_w/w \geq 2.0$ $U = 0.50 + 0.25L_w/w$, when $1.0 \leq L_w/w < 2.0$ $U = 0.75L_w/w$, when $L_w/w < 1.0$	No restrictions
AISC 360-10 Specification for Structural Steel Buildings	$U = 1 - \bar{x}/L_w$, $\bar{x} = \frac{B^2 + 2BH}{4(B+H)}$ $\bar{x} = \frac{3}{8}B$, when $B = H$	$L_w > H$
Martinez-Saucedo (2007) Slotted End Connections to Hollow Sections	$U = 1 - \frac{1}{\left[1 + \left(\frac{L_w}{w}\right)^{2.4}\right]^{5.7}}$	$L_w/w \geq 0.7$

2.2 Capacity Design

The braces of a CBF are expected to undergo alternating cycles of tension yielding and inelastic buckling during an earthquake. These ductile energy-dissipating mechanisms can only occur in a brace if the other components of the SFRS (connections, beams, columns etc.) are designed and detailed to accommodate the probable tensile and compressive resistances that are developed in the brace.

CSA S16 defines the probable tensile resistance of a brace as $R_yF_{ys}A_g$, where R_y is the ratio of expected yield stress to minimum yield stress, F_{ys} is specified minimum static yield stress, and A_g is the gross area of the tube. In CSA S16-09, the probable yield stress for HSS sections, R_yF_{ys}, is taken as not less than 460 MPa or that obtained from coupon testing in accordance with CSA G40.20 (CSA 2009b). The net-section resistance of a brace is defined as $(R_y/\phi_u)\ \phi_uA_{ne}F_{us}$, where R_y is taken as 1.2 for HSS sections, A_{ne} as defined before, and F_{us} is the minimum specified static ultimate stress. The R_y factor accounts for the expected increase in ultimate stress and can only be applied to net-section tensile resistance of a brace.

When applying these capacity design and net section requirements of CSA S16, $(R_y/\phi_u)\ \phi_uA_{ne}F_{us} > R_yF_{ys}A_g$ must be satisfied at the net section. When this is not possible, connection reinforcement must be used. Alternatively, the special MHG connection detail developed for circular tubes may be used. Before proceeding with such connection detail for square HSS connections, shear lag has to be properly understood for brace square tubular sections. Thus, one component of the experimental program is to examine existing shear lag design factors for conventional slotted square tube-to-gusset plate connections. These shear lag experiments will also provide a benchmark to compare with the performance of the MHG connections.

2.3 Strain Rate Effects

The dynamic yield-stress (F_{yd}) of steel increases with increasing strain rate, while the elastic modulus and stiffness in the strain hardening range remains generally unchanged (Wakabayashi et al. 1994). Tremblay and Filiatrault (1996) conducted shake table testing of a half-scale two-storey tension-only braced frame subjected to three earthquake records. The braces experienced strain rates of 17000 - 40000 με/s with an average strain-rate of 22000 με/s which gave F_{yd}/F_{ys} of 1.09 - 1.14 with an average of 1.12. The results compared favourably with the equation proposed by Wakabayashi et al. Also, the ratio of ultimate dynamic stress (F_{ud}) to ultimate static stress (F_{us}) was 1.02 - 1.07 with an average of 1.04.

This increase in yield stress is not considered in CSA S16 for calculating the probable brace tensile resistance. The experimental findings by Tremblay and Filiatrault (1996) suggest that the increase in F_{yd}/F_{ys} is more significant than F_{ud}/F_{us}; thus net-section fracture may occur before gross tube yielding even if a connection is satisfactorily designed using static stress values. Therefore, the effect of dynamic strain rates on connection behaviour are also investigated in this study, as outlined in Section 3.4.

3 EXPERIMENTAL PROGRAM

3.1 Specimen Designs

Two brace sizes, representative of lateral braces that are utilised in low- to medium- rise steel buildings were selected for this experimental program: HSS 152x152x9.5 and HSS 203x203x13.0 CSA G40.21 350W Class C (CSA 2009b). Before performing the connection designs, material properties (Table 2) were determined from coupons extracted from the flat portions of the tube (CSA 2009b).

Table 2: Measured Material Properties of HSS Specimens

Brace Size	F_{ys}[a] (MPa)	F_{us} (MPa)	F_{us}/F_{ys}
HSS 152x152x9.5	389	445	1.14
HSS 203x203x13.0	416	472	1.13

[a]Average of three coupons extracted from the flat portion of the tube and using the 0.2% offset method

The brace connection, for each of the two brace sizes, was designed for the tensile yield strength of the tube using the measured F_{ys} in accordance with CSA S16 capacity design principles. Firstly, a minimum possible weld length (L_w) was determined to prevent brace block-shear fracture. Using this weld length, a fillet weld (D_w) was selected to prevent weld- and base- metal fractures. This process was adopted since it was desired to see the maximum effect shear lag has on a brace net-section resistance while precluding other failure modes. Secondly, the Whitmore width was computed and a gusset plate thickness (t_g) was determined. Lastly, the net-section brace resistances were computed using the shear lag factors proposed by CSA S16, AISC and Martinez-Saucedo. Figure 3 shows a typical brace specimen while Figure 4 shows a magnified view of the brace-end connection detail for both brace sizes.

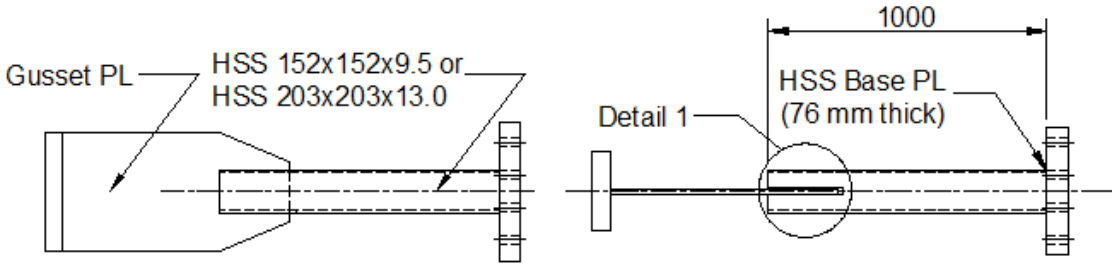

Figure 3: Typical specimen geometry

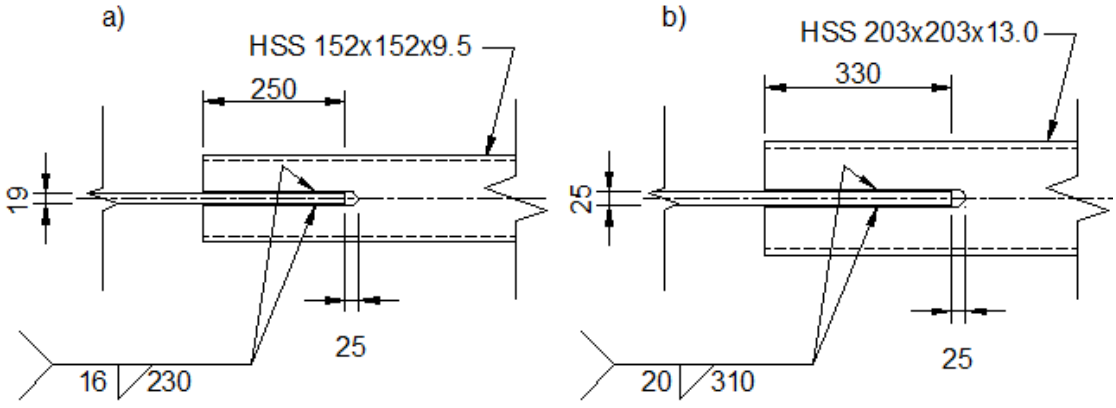

Figure 4: Slotted tube-to-gusset plate connection: a) HSS152x152x9.5, b) HSS 203x203x13.0

A total of four specimens were fabricated. Specimens 1 and 2 (HSS 152x152x9.5), as well as specimens 3 and 4 (HSS 203x203x13.0) were identical in fabrication. However, specimens 1 and 3 were tested under static rates, while specimens 2 and 4 were tested under dynamic rates. Table 3 shows the predicted net-section resistances for the statically loaded specimens. Specimens 1 and 3 were predicted to fail in net-section before gross tube yielding when the CSA S16 and AISC shear lag factors were used. On the other hand, both specimens were predicted to undergo gross tube yielding before net-section fracture when the shear lag factor proposed by Martinez-Saucedo (2007) was used.

Table 3: Predicted Net-Section Resistances for Specimens 1 and 3

Specimen #	Brace Size	Yield[a] Load $P_y=A_gF_{ys}$ (kN)	L_w/w	Shear-Lag Factors			Predicted Net-Section Resistances[b]		
				U_{CSA}	U_{AISC}	$U_{MARTINEZ}$	$\frac{T_{u,CSA}}{P_y}$	$\frac{T_{u,AISC}}{P_y}$	$\frac{T_{u,MARTINEZ}}{P_y}$
1	152x152x9.5	2027	0.92	0.69	0.75	0.97	0.72	0.79	1.02
3	203x203x13.0	3852	0.92	0.69	0.75	0.97	0.72	0.79	1.02

[a]Nominal areas were used. A_g = 5210 mm^2 and 9260 mm^2 for specimens 1 and 3 respectively
[b]Predicted brace resistances in accordance with CSA S16 and AISC determined with ϕ = 1.0

3.2 Setup

Each specimen consisted of a 1000 mm long HSS with a conventional slotted tube-to-gusset plate on one end and a 76 mm thick base plate (455 x 495) welded to the other brace end using a CJP and reinforcing fillet weld (Figure 3). The HSS base plate was bolted to a 102 mm thick T-Stub assembly base-plate using twelve 1-1/8"Ø ASTM A490 pre-tensioned bolts (Figure 5). The HSS and T-Stub assembly base plates were designed to remain elastic with no prying action.

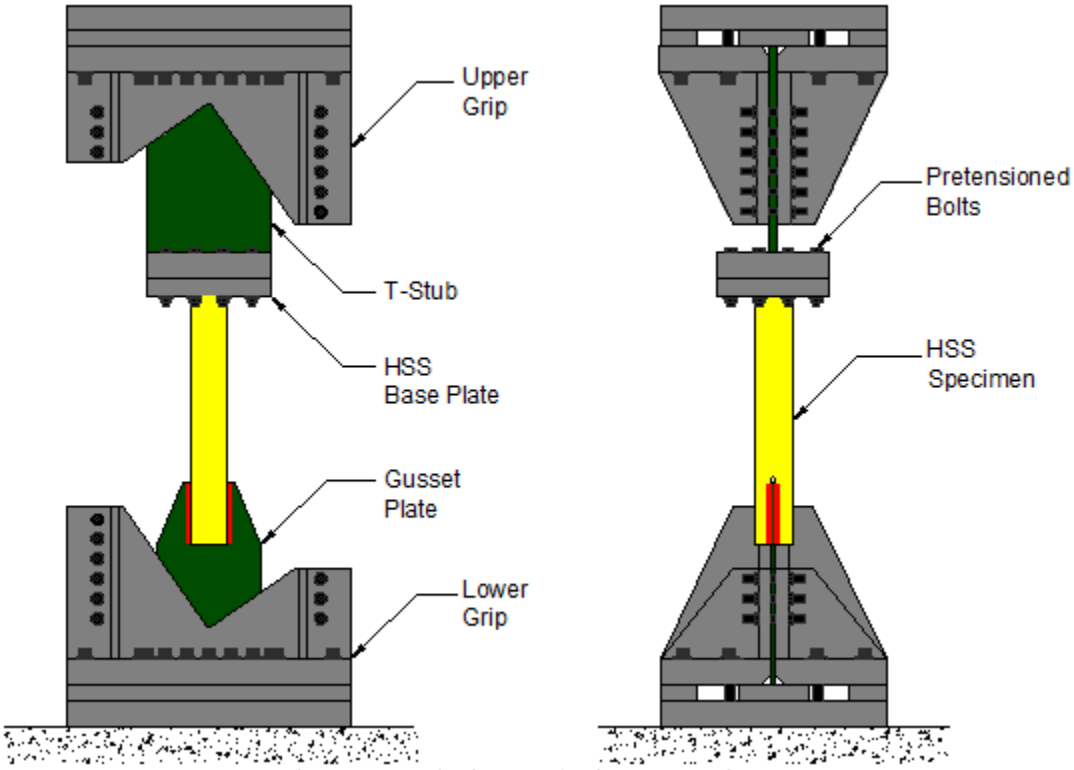

Figure 5: Typical setup for brace specimens

The gusset plate and T-Stub assembly were inserted into specially designed grips which were fastened to the upper and lower platens of the loading frame using high-strength pre-tensioned bolts. The upper platen was secured to a moveable cross-head of a double-acting, double-ended 12 MN actuator.

3.3 Instrumentation

The overall brace-displacement was measured using the average of two string potentiometers. These string potentiometers measured the displacement between the bottom of the HSS base plate and a distance of $2t_g$ from the tube end as seen in Figure 6a.

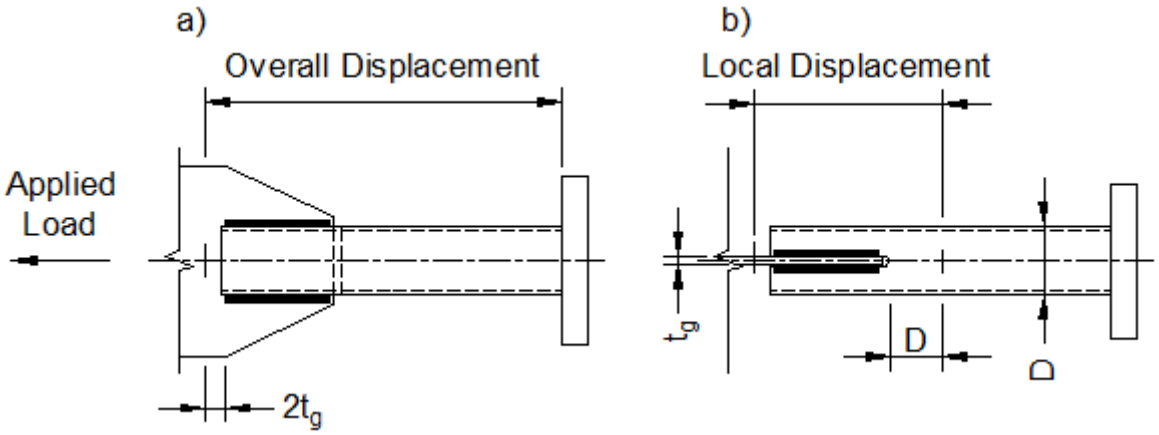

Figure 6: Location of string potentiometers used to measure displacements: a) Overall, b) Local

Similarly, string potentiometers were employed to measure the local connection displacements. These string potentiometers measured the displacements between $2t_g$ from the tube end to a distance equal to the depth of the section (D) away from the end of the tube slot (Figure 6b). This distance (D) was determined to be the tube length where the majority of the connection deformation was concentrated. This distance was determined using finite element modeling of the brace geometry. Additionally, a total of 15 strain gauges were located around the connection region and along the tube to measure the local strains.

3.4 Loading History

All specimens were tested in monotonic tension. The displacement of the HSS was controlled by the average of the two overall string potentiometers (Figure 6a), thereby allowing the strain rates in the HSS to be controlled. In order to prevent any strain-rate effects, the strains in the HSS were limited to 100 με/s for specimens 1 and 3 which gave an overall actuator piston speed of 0.004 mm/s. Detailed finite element analyses of the braces were conducted to determine the displacement rates.

Realistic estimates of the strains that are experienced in a brace during a design level earthquake were required. Izvernari (2007) conducted an analytical study to assess the performance of tension-compression CBF steel frames designed according to CSA S16. The response of five structures having between 2 and 16 storeys were examined using non-linear dynamic analyses under a suite of site specific ground motions.

The brace strain-rate histories were examined for selected braces. Strain rates varied between 33000 - 50000 με/s for when braces were subjected to large inelastic tension excursions. These strain rates were within the range observed experimentally by Tremblay and Filiatrault (1996). A brace strain-rate of 50000 με/s was selected for specimens 2 and 4 which gave an overall actuator piston rate of 50 mm/s for both specimens.

4 EXPERIMENTAL RESULTS

Table 4 shows the measured dimensions and geometric properties of the specimens. The measured gross area of the HSS was 1.7% and 2.9% less than the nominal area for HSS 152x152x9.5 and HSS 203x203x13.0 respectively. The weld lengths were on average 8% less than the specified weld lengths. This difference was due to the number of weld passes that were required to build the fillet welds. Nevertheless, the L_w/w values were consistent for all specimens.

Table 4: Measured Dimensions and Geometric Properties of Specimens

Specimen #	Brace Size	A_g[a] (mm^2)	A_n[b] (mm^2)	L_w[c] (mm)	D_w[d] (mm)	t_g (mm)	w (mm)	L_w/w
1	152x152x9.5	5123	4689	210	19.3	19.0	247	0.85
2	152x152x9.5	5123	4697	215	16.8	19.0	247	0.87
3	203x203x13.0	8991	8315	290	18.8	25.6	332	0.87
4	203x203x13.0	8991	8345	277	23.6	25.6	334	0.83

[a]Measured gross area by weighing a 250 mm long piece of tube and using a density of 7850 kg/m^3
[b]Measured net area by subtracting the A_g from the measured tube slot width and gusset plate thickness
[c]Average of weld length from two different sides of the gusset plate
[d]Average of weld leg sizes from two different sides of the gusset plate

4.1 Comparison of All Specimens

The normalised experimental-to-yield load vs. the overall brace-displacement for the HSS 152x152x9.5 and HSS 203x203x13.0 specimens are shown in Figures 7 and 8, respectively. All four specimens yielded on their gross cross-sectional before fracture on the net section. This is further confirmed by examining the strains that were developed in the gross cross-sectional area of the tube. The difference between the overall and local displacements (Figure 9) divided by that section of tube (L_{gross}) gives an indication of the tube strains. Table 5 lists the overall ($\Delta_{o,u}$) and local ultimate displacements ($\Delta_{l,u}$).The brace's gross strains are well above 2000 με indicating that gross tube yielding occurred. Unfortunately, the local displacements could not be recorded during the testing of specimen 2.

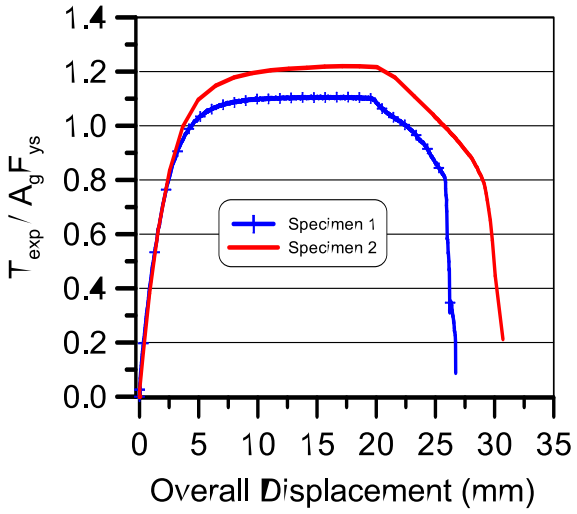

Figure 7: Normalised experimental load vs. overall displacement for HSS 152x152x9.5 specimens

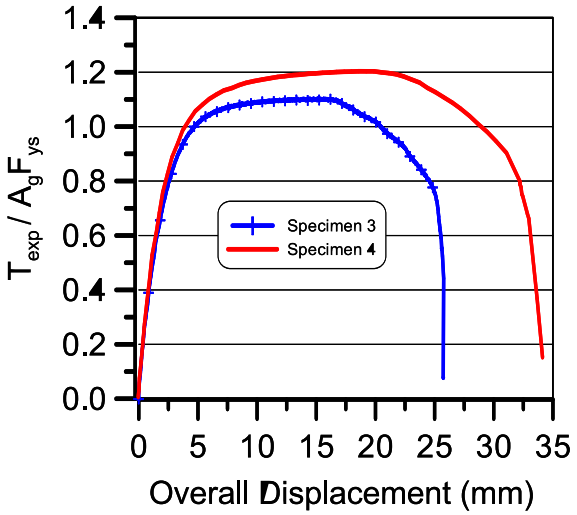

Figure 8: Normalised experimental load vs. overall displacement for HSS 203x203x13.0 specimens

Table 5: Brace Gross Strains for All Specimens

Specimen #	Displacement		Brace Gross Strain[a]
	Overall	Local	
	$\Delta_{o,u}$ (mm)	$\Delta_{l,u}$ (mm)	$\frac{\Delta_{o,u}-\Delta_{l,u}}{L_{gross}}$ (με)
1	19.5	14.1	9948
2	19.6	-	-
3	16.4	11.4	11312
4	20.4	12.9	16968

[a] L_{gross} = 573 mm (Specimens 1/2) and 442 mm (Specimens 3/4)

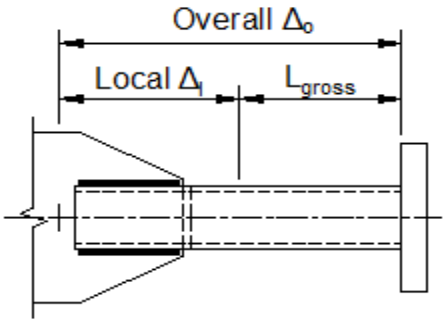

Figure 9: Brace Gross Strain Length

The dynamically loaded specimens experienced an increase in their ultimate load (T_{ud}) compared to their statically loaded counterparts (T_{us}). The T_{ud}/T_{us} was 1.10 and 1.09 for the HSS 152x152x9.5 and HSS 202x203x13.0 specimens respectively (Figures 7 and 8). Furthermore, the dynamically loaded specimens experienced greater ductility than the statically loaded specimens. This is indicated by the greater area under the load-displacement curve (Figures 7 and 8), as well as the higher brace gross strains (Table 5).

All specimens fractured in the net section with cracking initiating at the beginning of the weld and propagating circumferential around the tube as seen as in Figures 10 and 11. Additionally, extensive yielding was observed near the connection region as seen by tube necking (Figures 10c,e), white wash flaking off (Figures 10c,d and 11a,b), and elongation of the tube slot (Figures 10c,e and 11a,d).

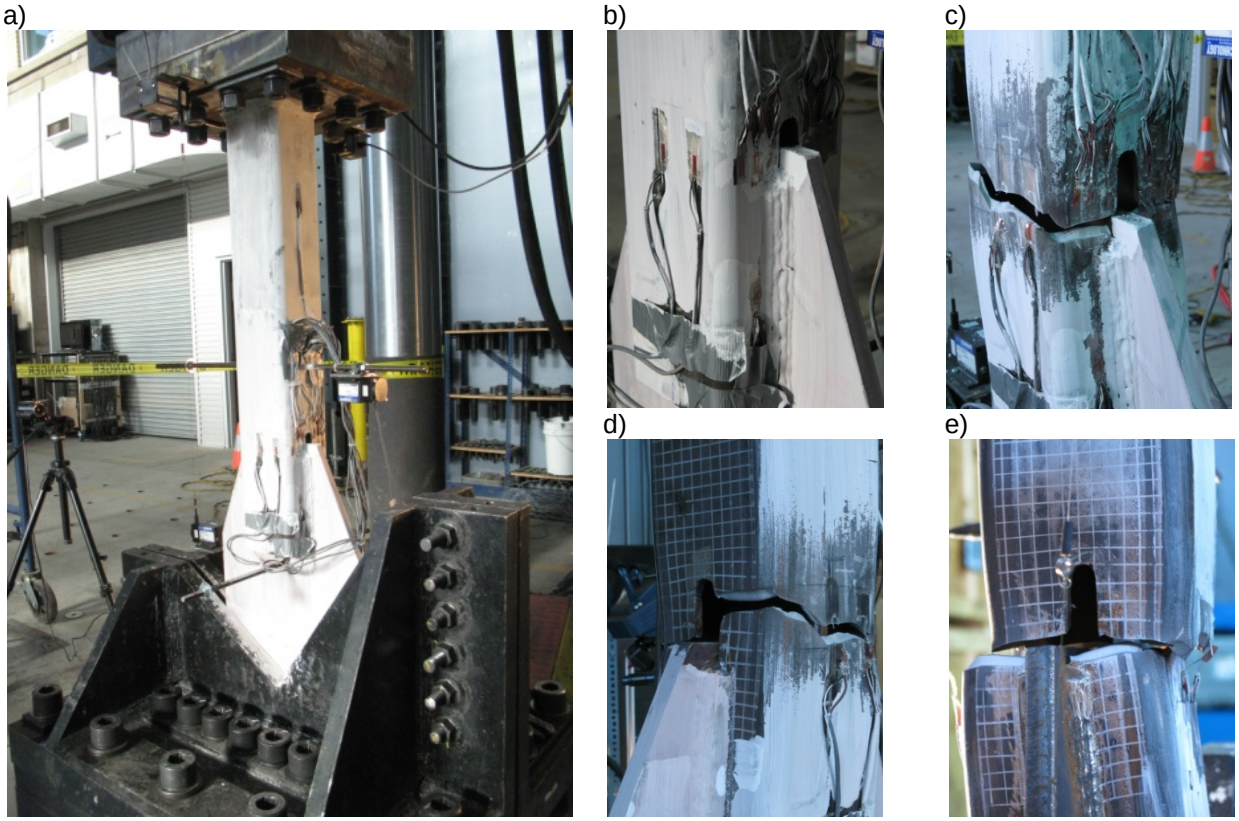

Figure 10: Typical brace specimen setup (a). Close-up views of the slotted tube-to-gusset plate connections showing net-section fracture for specimens 1 (b,c,d) and 2 (e)

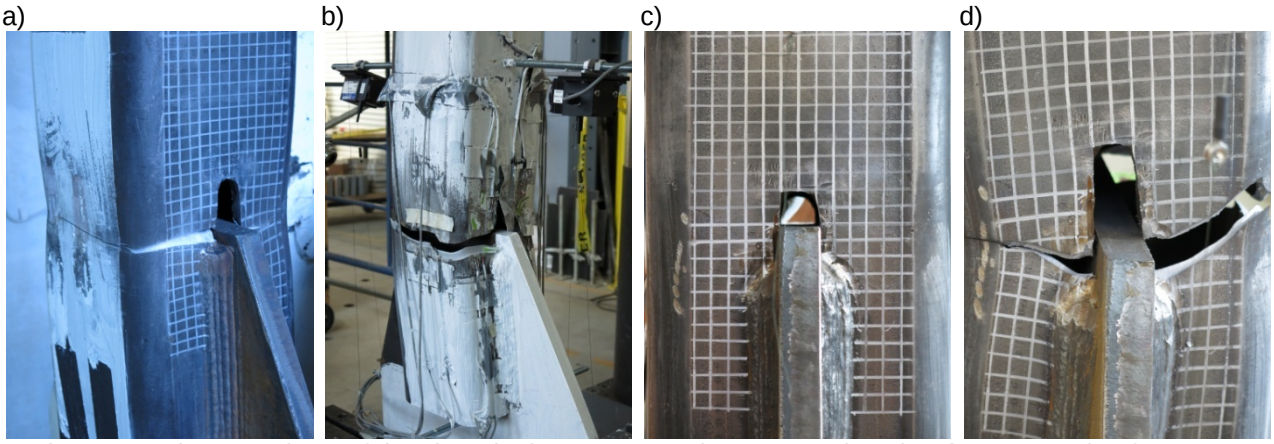

Figure 11: Close-up views of the slotted tube-to-gusset plate connection showing net-section fracture for specimens 3 (a) and 4 (b,c,d)

4.2 Comparison of Experimental and Predicted Brace Resistances

Table 6 shows a comparison of the predicted and experimental brace resistances using measured geometric and tube properties. As seen in Table 3, all specimens were predicted to fail by net-section fracture before tube yielding when the CSA S16 and AISC shear lag factors were used. However, all brace specimens yielded on their gross area before fracture. The net-section resistances were severely under-predicted when CSA S16 and AISC shear lag factors were applied. For the static tests, predictions by Martinez-Saucedo (2007) were on average 10% lower than the experimental loads. Net-section resistance predictions were conservative when the shear lag factor (U) was set to 1.0. This can be explained by the variability in the ultimate stresses from the coupon samples, as well as the likely (not measured) increase in material strength of the tube corners.

Table 6: Comparison of Predicted and Experimental Brace Resistances

Specimen #	Yield Load	Predicted Net-Section Resistances					Experimental Load ($T_{u,Exp}$) / Predicted Net-Section Resistances				
	P_y[a]	A_nF_{us}	T_{CSA}[b]	T_{AISC}[b]	$T_{MARTINEZ}$	$T_{u,Exp}$	$\frac{T_{u,Exp}}{P_y}$	$\frac{T_{u,Exp}}{A_nF_{us}}$	$\frac{T_{u,Exp}}{T_{CSA}}$	$\frac{T_{u,Exp}}{T_{AISC}}$	$\frac{T_{u,Exp}}{T_{MARTINEZ}}$
	(kN)	(kN)	(kN)	(kN)	(kN)	(kN)					
1	1997	2085	1331	1519	1976	2211	1.11	1.06	1.66	1.46	1.12
2	1997	2089	1362	1535	1992	2435	1.22	1.17	1.79	1.59	1.22
3	3743	3922	2567	2893	3744	4131	1.10	1.05	1.61	1.43	1.10
4	3743	3936	2452	2855	3702	4512	1.20	1.15	1.84	1.58	1.22

[a]Yield load was calculated using measured tube F_{ys} and A_g
[b]Predicted brace resistances with CSA S16 and AISC determined with $\phi = 1.0$

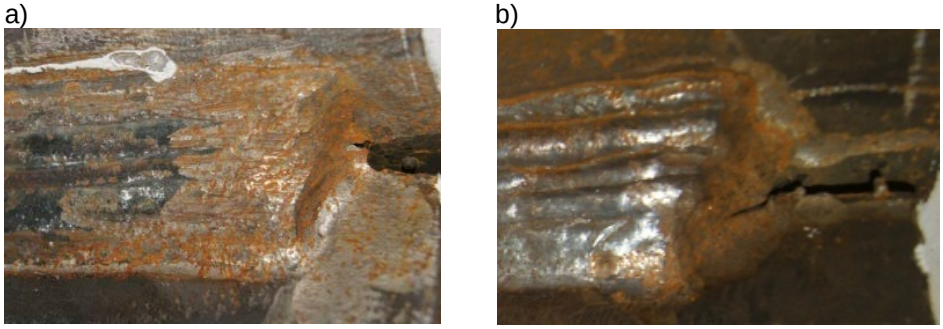

Figure 12: Initiation of tube-to-gusset plate weld fracture: a) Specimen 2, b) Specimen 4

The initiation of weld fracture at the tube-to-gusset plate interface was observed for the dynamically loaded specimens 2 and 4 (Figure 12). No noticeable weld distress was observed for specimens 1 and 3.

5 CONCLUSION

The HSS tubes used in this experimental program yielded on their gross area before net-section fracture without any connection reinforcement. The net-section brace resistances predicted by current CSA S16 and AISC provisions were found to be conservative for the test specimens. Shear lag predictions for circular tubes by Martinez-Saucedo agree reasonably well with experimental findings. The dynamically loaded specimens showed higher yield and ultimate strengths, as well as higher ductility than the statically loaded specimens. Furthermore, the initiation of weld fracture was observed for the dynamically loaded specimens.

ACKNOWLEDGEMENTS

The fabrication, technical and financial support provided by ADF Group Inc. and DPHV Structural Consultants is greatly appreciated. Also, this research project was funded by the Natural Sciences and Engineering Research Council of Canada (NSERC). The donation of the HSS tubes by Atlas Tube is gratefully acknowledged. The authors also wish to thank the technical staff of the Hydro-Quebec Structural Engineering Laboratory at Ecole Polytechnique of Montreal.

REFERENCES

AISC. 2010a. *Seismic Provisions for Structural Steel Building, ANSI/AISC 341-10*. American Institute of Steel Construction: Chicago, IL, USA.

AISC. 2010b. *Specification for Structural Steel Buildings, ANSI/AISC 360-10*. American Institute of Steel Construction: Chicago, IL, USA.

Cheng, JJR. and Kulak, G.L. 2000. Gusset plate connection to round HSS tension members. *Engineering Journal/ Fourth Quarter* : 133-139.

CSA. 2009a. *Design of Steel Structures S16-09*. Canadian Standards Assoc.: Mississauga, ON, Canada.

CSA. 2009b. General requirements for rolled or welded structural quality steel / structural quality steel G40.20/G40.21. Canadian Standards Assoc.: Mississauga, ON, Canada.

Fell, B.V. and Kanvinde, A.M. 2010. Tensile forces for seismic design of braced frame connections - Experimental results. *Journal of Constructional Steel Research*, 66: 496-503.

Izvernari, C.B. 2007. The seismic behaviour of steel braces with large sections. MSc. Thesis, University of Montreal, Ecole Polytechnique of Montreal.

Martinez-Saucedo, G. 2007. Slotted End Connections to Hollow Sections. Ph.D Thesis, University of Toronto.

Martinez-Saucedo, G., Packer, J. A., and Christopoulos, C. 2008. Gusset Plate Connections to Circular Hollow Section Braces under Inelastic Cyclic Loading. *J. of Structural Engineeri*ng, 134 (7): 1252-1258.

Tremblay, R., Filiatrault, A. 1996. Seismic Impact Loading in Inelastic Tension-only Concentrically Braced Steel Frames: Myth or Reality? Earthquake Engineering and Structural Dynamics, 25(12): 1373-1389.

Tremblay, R., Bruneau, M., Nakashima, M., Prion, H. G. L., Filiatrault, A., and Devall, R. 1996. Seismic design of steel buildings: lessons from the 1995 Hyogo-ken Nanbu earthquake. *Canadian Journal of Civil Engineerin*g, 23: 727-756.

Wakabayashi, M., Nakamura, T., Iwai, S., and Hayashi, Y. 1994. Effects of strain rate on the behavior of structural members. *In 8th World Conference on Earthquake Engineering*, San Francisco, LA, USA, vol.4 : 491-498.

Willibald, S., Packer, J.A., Martinez-Saucedo, G., and Puthli, R.S. 2004. Shear Lag in Slotted Gusset Plate Connections to Tubes. *In Proc. Connections in Steel Structures V*, Amsterdam: 445-456.

Yang, F. and Mahin, S. 2005. Limiting Net Section Fracture in Slotted Tube Braces. *Steel Tips*, Structural Steel Education Council, Moraga, CA.